Available online at www.sciencedirect.com
ScienceDirect
Coastal Engineering 53 (2006) 857–864
Coastal Engineering
An International Journal for Coastal, Harbour and Offshore Engineers
www.elsevier.com/locate/coastaleng

Multi-point tidal prediction using artificial neural network with tide-generating forces

Hsien-Kuo Chang *, Li-Ching Lin

Department of Civil Engineering, National Chiao-Tung University, Hsinchu 300, Taiwan

Received 19 September 2005; received in revised form 23 February 2006; accepted 1 May 2006
Available online 23 June 2006

Abstract

This paper presents a neural network model of simulating tides at multi-points considering tide-generating forces. A comparison on the root mean square and correlation coefficient of three-year mixed tides at a single point computed with harmonic method, response–orthotide method, the NAO.99b model and the proposed model was made to show the prediction accuracy of each method. The proposed model is examined efficient as the harmonic method to estimate the tides at a single point. Extended application of the proposed model to predicting tides at some points neighboring to an original interest point identifies accurately simulating multi-point tides as the NAO.99b numerical model.

Keywords: Neural networks; Tides; Tide-generating forces; Harmonic method

1. Introduction

The oceanic tide refers to the rhythmic rise and fall of sea level with time made evident at a coast by the periodic advancing and receding of the waters from the shore. Tidal motions tend to get amplified (or reduced) across broad shelves, and response to meteorological conditions more vigorously than those in deep water. In shallow water, local effects can modify tidal constituents particularly by producing harmonics whose frequencies are simple multiples of the frequency of the constituent concerned. These harmonics result from frictional interaction between the sea bed and the ebb and flow of the tide. Coastlines can reflect tidal waves to make actual tides in a specific area higher or lower than expected by the astronomical forcing. The combined constraint of ocean basin geometry and the influence of the Coriolis force results in the development of amphidromic systems, in each of which the crest of the tidal wave at high water circulates around an amphidromic point once during each tidal period. Although the interactions of all the forces and factors are so complex that the coastal tide times and ranges on the shore, the coastal tide could not be very accurately predicted. In coastal engineering, calculating tidal level can decide a design level for the top of marine structures and the safe ship navigation in a harbor. An expected accurate prediction of tidal levels becomes of importance for coastal engineering and marine navigation.

The harmonic method (abbreviated HM) developed by Darwin (1907) assumes that the tides can be regarded as superposition of different harmonics whose frequencies are known from astronomy (Doodson, 1921; Desai, 1996). The information can then be used to provide reliable predictions for future tides at the same point. The remarkably good accuracy of these predictions impresses researchers understanding of how the tide behaves in the ocean. The length of record needed to extract different components depends primarily on the closeness in frequency of the components that are to be extracted and on the lowest frequency of the components chosen. Normally, 369 days of hourly data at a point are needed to extract 20 to 30 constituents with adequate separation of closely spaced constituents using the least squares method. Le Provost et al. (1998) used 26 major constituents in their numerical model.

The disadvantage of HM can be solved by the inherent smoothness of the admittance function, which acts on the tide-generating, giving the observed tide as its output. Tidal constituents that are closely spaced to one another and hence have essentially the same admittance function are treated independently of one another. It is possible to take advantage of the

* Corresponding author. Fax: +886 3 513 1487.
E-mail address: hkc@faculty.nctu.edu.tw (H.-K. Chang).

0378-3839/$ - see front matter © 2006 Elsevier B.V. All rights reserved.
doi:10.1016/j.coastaleng.2006.05.001

inherent smoothness of the tidal response function to make accurate tidal prediction with a smaller number of constituents (Munk and Cartwright, 1996; Groves and Reynolds, 1975). The response–orthotide method (abbreviated R-O) is introduced in detail by Ray (1998) and Desai (1996) and is often preferred in the tidal models for estimating the linear tides in the global oceans, such as Desai and Wahr (1995), Han et al. (2000), Matsumoto et al. (2000). Both HM and R-O are applicable for tidal predictions only for one point where observed data are used to determine unknown constants.

Nevertheless, R-O explains that the actual tides depend on the tide-generating forces. The resulting conclusion implies that there is a comparable relationship existing between actual tides and tide-generating forces. If the relationship can be established, computed tide-generating forces by astronomy can be used to estimate the tides through the well established relationship.

The paper addresses an efficient tool of artificial neural network (ANN) to obtain the relationship between actual tides and tide-generating forces. ANN has high functioning with fast computation and a considerable memory to solve the problems concerning extremely nonlinear interactions and complex effective variables. Accordingly, ANN has newly been implemented widely in different areas. Some examples of using neural network in marine engineering and science are demonstrated by Vaziri (1997), Deo and Shidhar Naidu (1998), Tsai and Lee (1999), Deo et al. (2002), Lee and Jeng (2002), Lee et al. (2002), Makarynskyy (2004), Lee (2004) and Chang and Chien (2006, in press), etc.

For particular application of ANN to tidal prediction, Vaziri (1997) presents both ANN model and ARIMA model for predicting Caspian Sea surface water level. Tsai and Lee (1999) applied an ANN model to forecast the tidal levels of diurnal and semidiurnal tides without determining the harmonic parameters. Later four discussions by Kumar and Minocha (2001), Mandal (2001), Medina (2001) and Walton and Garcia (2001) on the paper of Tsai and Lee (1999) were raised some practicality and theoretical issues. One of the disadvantages is that the application of the ANN model of Tsai and Lee (1999) gives only one-hour tidal predictor due to the sequentially observed tidal data required as inputs of which the lead time is 1 h. Lee et al. (2002) employ an application of ANN for predicting and supplementing the tidal level using short term observed data. Lee and Jeng (2002) developed an ANN model associated short term measured data in the learning stage to provide a long term predictor in tides. The drawback of the ANN model of Lee and Jeng (2002) is that it needs several lead time tidal data observed to be input in the ANN model for predicting sequential tides. These ANN tidal models are limited to a single point tidal predictor.

Matsumoto et al. (2000) developed a global ocean tidal model, which is called NAO.99b, for 16 major short period constituents by assimilating about five years of *T*/*P* altimeter data into numerical hydrodynamical model. NAO.99b is examined to have comparable agreement with many tide gauge data as well as CSR4.0 and GOT99.2b. The accuracy of simulation on tides by NAO.99b is confirmed so that NAO.99b is widely accepted and used to evaluate the accuracy of simulating tides using the proposed ANN model.

The authors use tide-generating forces of astronomy as inputs in the proposed ANN model to establish the valid relationship between tides and tide-generating forces. Thus the proposed model is named by TGF-NN. TGF-NN is compared with the commonly accepted HM to have accurate estimation on tides at a single point. Furthermore, TGF-NN is extended to predict the tides at some points neighboring the point where tidal data are used to develop TGF-NN. For engineering practices the proposed TGF-NN can be used to estimate tides at a point, where tide station is not established to collect tide data and some observed data can be available from a neighboring point.

2. Tide-generating potential

Oceanic tides are mostly the combined result of the gravitational attraction between the earth and the moon, and the gravitational attraction between the earth and the sun. Tides due to other planetary bodies are negligible. For gravitational purposes, a geocentric coordinate system shown in Fig. 1 is considered to conveniently describe the tides in the earth. In this coordinate system, the gravitational potential at any point P on the earth's surface with a vector $\mathbf{r}$ due to a mass M of the body at another point with a vector $\mathbf{r}$ is given (Lamb, 1945) as

$$\phi_a = \frac{GM}{|\mathbf{d}|} \tag{1}$$

where $G \approx 6.67 \times 10^{-11}$ Nm/kg^2 is the coefficient of universal gravitation; $R = |\mathbf{r}| \approx 6.371 \times 10^6$ m is the radius of the earth; D is the distance between the earth's center and the center of the body; $\xi = |\mathbf{d}|$ is the distance between the point P and the center of the body. This gravitational potential causes gravitational force $F_a = GM/\xi^2$ which points towards the center of the body.

The centrifugal force due to the mutual rotation of two bodies shown in Fig. 1 at any point on the earth opposite pointing towards $\mathbf{d}$ is given as

$$F_c = \frac{GM}{D^2} \tag{2}$$

The radial component of the centrifugal force at point P is $F_c \cos\theta$ and the tangential component is $F_c \sin\theta$ where θ is the

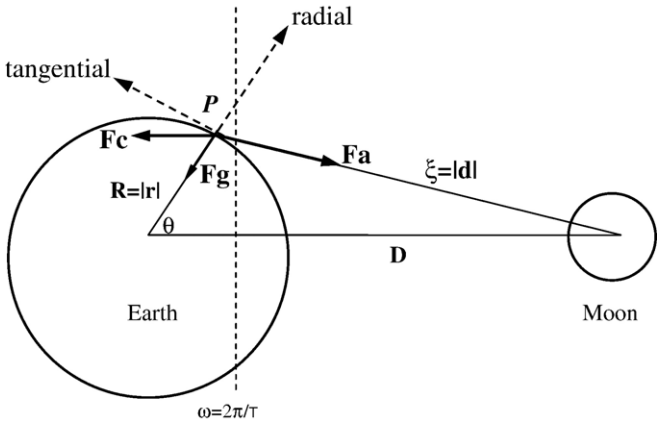

Fig. 1. Geometry of gravitational force and centrifugal force on a point P at the surface of the earth.

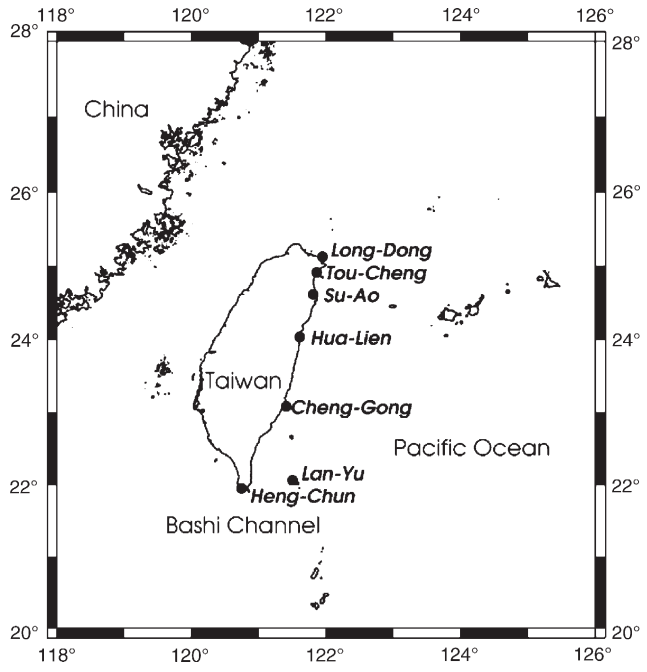

Fig. 2. Location of tidal gauge observed.

angle between two vectors, **r** and **d**. A potential, ϕ_c, can be related to the centrifugal force and given as

$$\phi_c = -\frac{GM}{D^2} r\cos\theta + \phi_0 \tag{3}$$

where ϕ_0 is an integral constant that can be determined by a resulting tidal potential $\phi=\phi_a+\phi_c$ specified. Assuming zero tidal potential at the earth's center, that is $\phi=0$ at $r=0$, $\theta=0$ and $\xi=D$, $\phi_0=-GM/D$ is then decided. The resulting tidal potential due to tidal generating forces at the point P on the earth's surface is thus obtained

$$\phi = GM\left(\frac{1}{\xi}-\frac{R\cos\theta}{D^2}-\frac{1}{D}\right) \tag{4}$$

The simple theory of the oceanic response to tidal potential is that the ocean is taken a shape which keeps its surface in instantaneous gravitational equilibrium with the combination of tidal accelerations and the earth's gravity. In this equilibrium theory, ocean surface is one of uniform total gravitational potential. Neglecting the nonlinear interaction between all possible components of the tidal potential, the tidal displacement of the oceanic free surface due to a body is then expressed as

$$\eta \approx -\frac{\phi}{g} = -\frac{GM}{g}\left(\frac{1}{\xi}-\frac{R\cos\theta}{D^2}-\frac{1}{D}\right) \tag{5}$$

where g is the acceleration due to the gravity of the earth. Considering both the solar and lunar tides, Eq. (5) results in equilibrium tides

$$\eta_e = -\frac{GM_m}{g}\left(\frac{1}{\xi_m}-\frac{R\cos\theta}{D_m^2}-\frac{1}{D_m}\right)-\frac{GM_s}{g}\left(\frac{1}{\xi_s}-\frac{R\cos\theta}{D_s^2}-\frac{1}{D_s}\right) \tag{6}$$

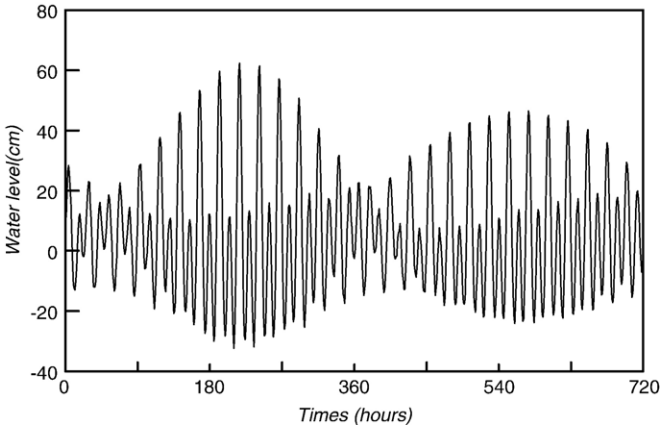

Fig. 3. Equilibrium tides computed by Eq. (6) at the Hua-Lien for Jan. 2001.

where the subscripts of m and s denote the physical quantity corresponding to the moon and the sun, respectively; the mass of the moon is $M_m \approx 7.38\times10^{22}$ kg and the mass of the sun is $M_s \approx 1.989\times10^{30}$ kg; the distance between these two bodies is $D_m \approx 3.84\times10^{8}$ m and the earth itself orbits around the sun once a year by a mean distance $D_s \approx 1.495\times10^{11}$ m. The solar tide computed by Eq. (6) due to the sun's gravitational force is about 0.459 times that of the moon. When the values of ξ, θ and D at any time of some locations around Taiwan are obtained by astronomy, the equilibrium tides can be obtained by Eq. (6). Seven locations are chosen and plotted in Fig. 2.

The equilibrium tides computed by Eq. (6) and observed tides at the Hua-Lien which is located at the central coast of eastern Taiwan and shown in Fig. 2 for January 2001 are depicted in Figs. 3 and 4, respectively. Visual comparison on tides of Figs. 3 and 4 illustrates that although the tidal range and diurnal inequality of the equilibrium tides and observed tides are significantly different, the neap-spring tidal cycle is almost in phase.

3. The construction of back-propagation neural network

The back-propagation network (BPN) with multiple-layer networks and nonlinear differentiable transfer functions is popularly used to solve many problems whose solutions that need optimization. Input vectors and the corresponding target vectors

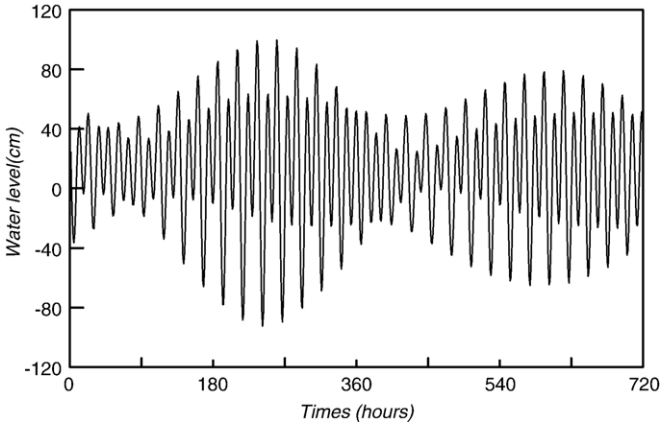

Fig. 4. Observed tides at the Hua-Lien for Jan. 2001.

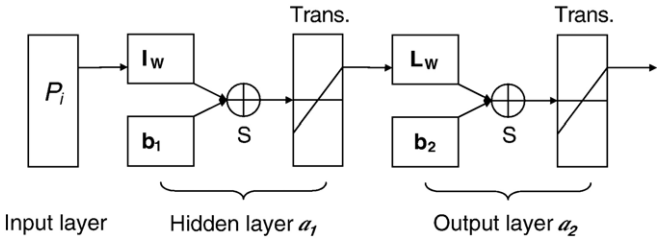

Fig. 5. Sketch of the construction of back-propagation network.

are used to train a BPN, until it can approximate a function that associates the input vectors with specific the output vectors. Networks with biases, a sigmoid layer and a linear output layer can approximate any function with a finite number of discontinuities (Demuth and Beale, 2000). A properly trained BPN tends to generate reasonable answers when inputs are provided with it. Therefore, the back-propagation algorithm is an extensively used algorithm in neural networks. TGF-NN is established using the neural network toolbox of the *MATLAB* software and is shown in Fig. 5.

The symbol P_i in Fig. 5 is the input vector, and $\mathbf{I}_w$ and $\mathbf{b}_1$ are the matrices of weights and of biases between the input neurons and the hidden layer neurons, respectively, *Trans.* is the transfer function, and $\mathbf{L}_w$ and $\mathbf{b}_2$ are the matrices of weights and biases between the output neurons and the hidden layer neurons, respectively. The connections between the input neurons and hidden layer neurons, and those between the hidden perceptions and outputs can be formulated as the following equations

$$\mathbf{a}_1 = f(\mathbf{I}_w P_i + \mathbf{b}_1) \tag{7}$$

and

$$\mathbf{a}_2 = f(\mathbf{L}_w \mathbf{a}_1 + \mathbf{b}_2) \tag{8}$$

where $\mathbf{a}_1$ is the value of the first hidden layer; $\mathbf{a}_2$ is the output value of the network, and $f(x)=2/(1+e^{-2x})-1$ is the hyperbolic tangent sigmoid transfer function. For sigmoid units, the output varies continuously but not linearly as the input changes. Thus sigmoid units bear a greater resemblance to real neurons than do the other two kinds, linear or threshold units.

Networks with biases can present relationships between inputs and outputs more easily than can networks without biases. Accordingly, a bias matrix in TGF-NN is considered. TGF-NN consists of one input layer, one hidden layer and one output layer. The supervised learning rule is applied to modify the weights and biases of a network by comparing the outputs to the targets when the inputs are applied to the network. The new values of all elements of the weight and the bias matrices must be checked by computing the network outputs for each input vector to determine whether all targets are reached.

The squared difference between the desired response $\mathbf{Y}$ and the network response $\mathbf{a}_2$ states the learning error or training error, E, and can be written as

$$E = \frac{\|\mathbf{a}_2 - \mathbf{Y}\|^2}{N} \tag{9}$$

where N is the total number of data and $\|\mathbf{a}_2-\mathbf{Y}\|$ is the norm of the vector $\mathbf{a}_2-\mathbf{Y}$.

When the learning error E is less than a specified tolerance, of which the value is 10^{-5} used in this paper, the iteration terminates. This study uses the Levenberg–Marquardt (L-M) algorithm to determine the weight and the bias matrices in the each iteration. An approximation to the Hessian matrix in a Newton-like update is used for the L-M algorithm as follows

$$\mathbf{X}_{k+1} = \mathbf{X}_k - [\mathbf{J}^T\mathbf{J} + \mu\mathbf{I}]^{-1}\mathbf{J}^T\mathbf{e} \tag{10}$$

where $\mathbf{X}_k$ and $\mathbf{X}_{k+1}$ represent the time steps that precede and follow an iteration, respectively; $\mathbf{J}^T$ is the transpose matrix of $\mathbf{J}$; $\mathbf{I}$ is the identity matrix, and μ and $\mathbf{e}$ are a small value and the error matrix at time t. When μ is zero, Eq. (10) specifies Newton's method, using an approximate Hessian matrix. When μ tends to be large, Eq. (10) becomes the gradient descent method, with a small step size. Thus, performance function will always be reduced at each iteration of the algorithm (Gill et al., 1981).

The input parameters D, ξ and θ between the sun and the earth and between the moon and the earth at any time are key parameters for determining tide behavior. The angle φ between two vectors from the center of the earth to the center of the sun and moon determines the relative positions of the sun, the moon and the earth. When the moon and the sun are on the same or opposite side of the earth, that is, $\varphi=\pm\pi$, the tides are the largest and are known as high spring tides. When the sun and the moon are perpendicular, the tides are lowest and are called low neap tides. Spring tide occurs when $\cos\varphi=\pm1$. Neap tide arises when $\cos\varphi=0$. Thus, the $\cos\varphi$ can be adopted to identify the spring-neap tidal cycle.

From Eq. (5) equilibrium tides relate to $1/\xi$, $\cos\theta/D^2$ and $1/D$. Although real tides are possibly influenced by local effects, such as ocean basin geometry, frictional interactions, boundary reflection etc., tide-generating forces play an important role in the rise and fall of real tides. Therefore, real tides respond to the tide-generating forces of which the expression can be chosen as the input parameters in the ANN model. The seven crucial parameters, $R/D_m(t)$, $R/D_s(t)$, $R/\xi_m(t)$, $R/\xi_s(t)$, $[R/D_m(t)]^2\cos\theta_m(t)$, $[R/D_s(t)]^2\cos\theta_s(t)$ and $\cos\varphi(t)$, form an input vector and are related to the output, observed tides at the Hua-Lien, in TGF-NN to establish the valid weight and bias matrices. The proposed model has one hidden layer with five neurons. The number of neurons was determined by examining several cases of different numbers of neurons in the hidden layer, and selecting the number leading to the smallest target error. The maximum iteration was set to 1500 in the optimal procedure.

Some advanced architectures and learning schemes like RBF and ANFIS are available. The neurons of RBF only respond to relatively small regions of the input space. The larger the input space is the more RBF neurons are required. The proposed input matrix is [21*8760] when 21 inputs and 8760 data are used. ANFIS provides membership functions with some inputs to establish the fuzzy rules having M^I where M is the number of membership functions and I is the number of inputs (Atsalakis et al., 2005). If 2 membership functions are used in the TGF-NN which has 21 inputs, thus there are 2^{21} fuzzy rules. Therefore, huge memory and computation time are required for training ANFIS. However, it is possibly applicable for any potential

Table 1
Annual RMS and r^2 between modeled and observed tides at the Hua-Lien (unit: cm)

Year	RMS	HM(60)	TGF-NN (lead time)			
	r^2	–	3	2	1	0
2001	RMS	6.57	8.43	6.37	8.64	17.58
	r^2	0.975	0.955	0.976	0.933	0.843
2002	RMS	10.28	14.45	10.57	13.02	15.75
	r^2	0.939	0.867	0.935	0.874	0.832

researcher to apply RBF or ANFIS to this problem for comparing the predictions with the proposed TGF-NN model.

4. Model validity

4.1. Simulating tides at an interest point

Commonly the simulation performance of predictors by a model is evaluated by the root mean square (RMS) or the square of correlation coefficient (r^2) (see Kleinbaum et al., 1988). The RMS and r^2 are defined as

$$\mathrm{RMS} = \sqrt{\frac{\sum_{i=1}^{N}[\eta_m(t_i)-\eta_p(t_i)]^2}{N}} \tag{11}$$

and

$$r^2 = \frac{\sum_{i=1}^{N}[\eta_m(t_i)-\bar{\eta}_p]^2 - \sum_{i=1}^{N}[\eta_m(t_i)-\eta_p(t_i)]^2}{\sum_{i=1}^{N}[\eta_m(t_i)-\bar{\eta}_p]^2} \tag{12}$$

where $\eta_m(t_i)$ and $\eta_p(t_i)$ are the measured and calculated tidal levels, respectively, at time t_i; $\bar{\eta}_p$ is the mean of all predictors. r^2 varies from zero to one. Small RMS and large r^2 indicate that the simulation performance is good.

The tidal data at the Hua-Lien were applied to assess the simulation accuracy of TGF-NN. The mean spring tidal range and mean overall tidal range at the Hua-Lien are 1.99 m and 1.06 m, respectively. One-year tidal data in 2001 were used to find the coefficients in HM(60) and to train TGF-NN. The tidal data in next three years were utilized to study the simulating capacity of each method.

Tides move as long waves which propagate periodically in time. The tide at time t may be composed of previously sequential tidal waves. The probable lead time of tides was examined for TGF-NN. When the n-hour lead time was considered, the number of neurons in the input layer was set to $7n$. Table 1 displays the RMS obtained by HM(60) and TGF-NN considering the lead time effect, demonstrating that the proposed model with 2-hour lead time inputs had the smallest RMS = 6.37 cm and the largest $r^2 = 0.976$ among all cases in 2001. The corresponding RMS from predicting one-year tidal data in 2002 using TGF-NN was 10.57 cm, which is slightly larger than that obtained by HM(60) and significantly smaller than that of TGF-NN with different lead time inputs. The largest $r^2 = 0.935$ among all cases in 2002 is comparable to that by HM (60). Therefore, the proposed TGF-NN including one output neuron and one hidden layer with five neurons and seven-parameter input vector including 2-hour lead time effect was found to have comparable accuracy for calculating tidal levels compared with HM(60) and is suitably used for further application hereafter. The authors also use the raw causative variables to test the NN model and then find that the training error is worse than that of the TGF-NN model when dimensionless data are used in the proposed TGF-NN.

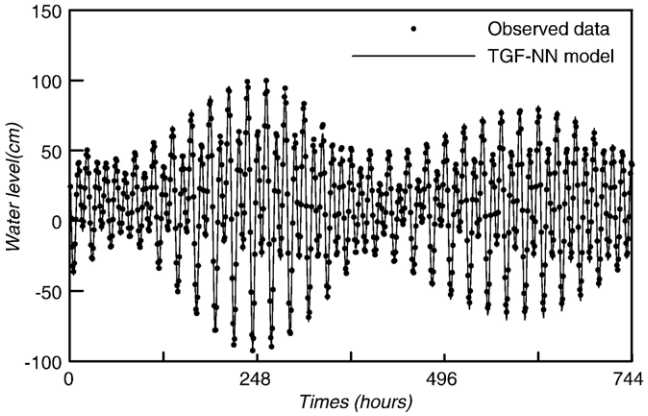

Fig. 6. Time history of simulated and observed tides at the Hua-Lien for Jan. 2001.

Time history and scatter plot of observed data and simulated tides by TGF-NN in training stage at the Hua-Lien for 2001 are depicted in Figs. 6 and 7, respectively. Small disparity between observed and simulated tides in Fig. 6 demonstrates a possibly narrow scatter plotted in Fig. 7 in which r^2 is 0.976. Figs. 8 and 9 show the time history and scatter plot for 2002 in the verification stage. A slightly wider scatter in Fig. 9 than that in Fig. 7 illustrates that TGF-NN has larger RMS in verification stage

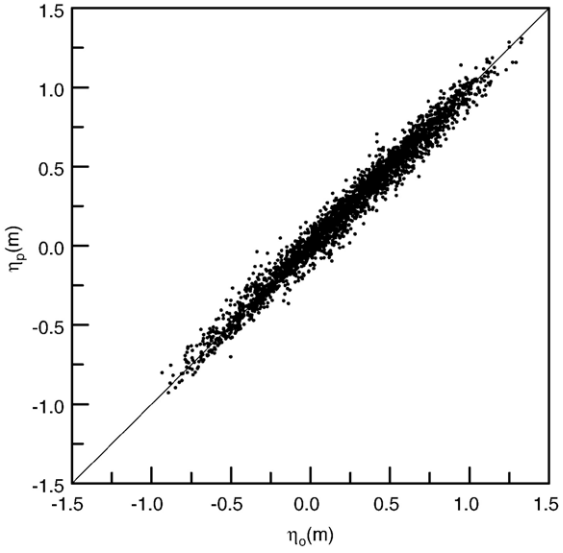

Fig. 7. Scatter plot of simulated and observed tides at the Hua-Lien for 2001.

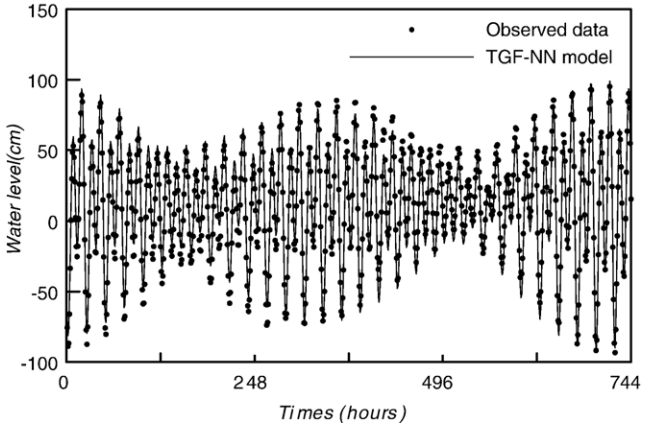

Fig. 8. Time history of simulated and observed tides at the Hua-Lien for Jan. 2002.

than in the learning stage. This is a common result in establishing an ANN model.

Table 2 lists the RMS and r^2 obtained by HM, R-O, NAO.99b and TGF-NN. The RMS and r^2 obtained by HM with 60 and 26 constituents are listed in the second and third rows, respectively. The RMS in the second column of Table 2 and r^2 in the sixth column from 2001 indicates that HM with 60 constituents and TGF-NN have similarly small RMS and large r^2. The RMS of simulated tides for the next three years listed in the third to fifth columns reveals that both HM with 60 constituents and TGF-NN have comparably high accuracy of simulating tides with RMS varying from 10.28–12.21 *cm*. Good simulations by HM and TGF-NN can be also established by comparing r^2 in the last three columns of Table 2. A comparison on RMS and r^2 in Table 2 shows that HM with 26 constituents, R-O and NAO.99b have comparable simulation on tides, but slightly worse than both HM with 60 constituents and TGF-NN. NAO.99b considers 16 main constituents at each grid in the tidal solutions and corrects the predicted tides using altimetry tidal data. Thus the simulation accuracy of NAO.99b is similar to that of HM with 26 constituents, because the tides at

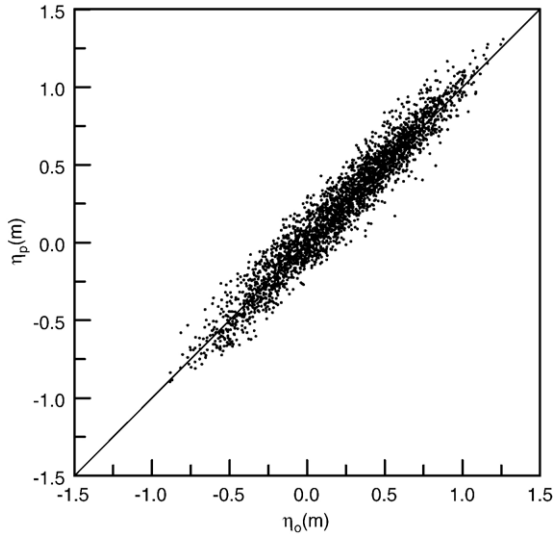

Fig. 9. Scatter plot of simulated and observed tides at the Hua-Lien for 2002.

Table 2
Annual RMS and r^2 between modeled and observed tides at the Hua-Lien for four years (unit: cm)

Method	RMS				r^2			
	2001	2002	2003	2004	2001	2002	2003	2004
HM(60)	6.57	10.28	12.21	10.38	0.975	0.939	0.964	0.937
HM(26)	15.21	11.34	10.35	13.76	0.866	0.917	0.909	0.888
R-O	15.24	11.28	10.34	13.52	0.865	0.918	0.938	0.891
NAO.99b	15.61	11.69	10.69	14.05	0.861	0.911	0.930	0.884
TGF-NN	6.37	10.57	11.70	11.96	0.977	0.935	0.954	0.919

the Hua-Lien are mixed but predominantly semidiurnal in a coastal region. TGF-NN addresses the tidal generating forces which can induce many possible constituents. Therefore, TGF-NN is proportionate to HM with many constituents. Normally, R-O is examined good to predict the amplitude and phase of main constituents when the short tidal record is employed. More tidal data in coastal regions in this study probably can not promote R-O worse for estimating tides. For application to a single point, TGF-NN is as powerful as the standard HM for estimating tides when trained with one-year tidal data.

4.2. Extension to predicting tides at neighboring points

The proposed model was developed using the tidal data at the Hua-Lien in the training procedure, and was examined to ensure that it would accurately simulate tides at the Hua-Lien at any time. The developed model is extended herein to six points neighboring to the Hua-Lien. Six points, Long-Dong (LD), Tou-Cheng (TC), Su-Ao (SA), Cheng-Gong (CG), Lan-Yu (LY), and Heng-Chun (HC), depicted in Fig. 2, at the eastern coast of Taiwan, are selected as the examined points. The Long-Dong, Tou-Cheng and Su-Ao are about 131, 106 and 72 km, respectively, north of the Hua-Lien. The Cheng-Gong, Lan-Yu and Heng-Chun are about 102, 214 and 243 km, respectively, south of the Hua-Lien. The Lan-Yu station is located at a small island away from eastern Taiwan by a distance of about 78 km.

Tides at a point can be either predominantly semidiurnal, predominantly diurnal, or mixed. Their nature is determined by the ratio $F=(K_1+O_1)/(M_2+S_2)$ where K_1, O_1, M_2 and S_2 are the amplitudes of four main constituents at a point in general. If $F<0.25$, the tides are predominantly semidiurnal and if $F>3.0$, the tides are predominantly diurnal. If $0.25<F<1.5$, the tides are mixed, but mainly semidiurnal, and if $1.5<F<3.0$, the tides are mixed, but mainly diurnal. The six points from north to south are examined to have $F=1.14$, 0.71, 0.64, 0.49, 0.42 and 1.18, respectively. $F=0.48$ is estimated for the Hua-Lien. All values of F at chosen points indicate mixed tides, but mainly semidiurnal. The mean tidal ranges at chosen points vary within a range of 65–109 cm.

Table 3 presents the RMS and r^2 of simulated tides at six points in 2001 and 2002 using NAO.99b and TGF-NN. The input parameter values were separately computed for the six points and inserted into the well developed model to directly output their tides. Tidal data at the Long-Dong for year 2001 are not available for estimating RMS. The difference of annual

Table 3
Annual RMS and r^2 between observed and predicted tides at six points (unit: cm)

Year	Index	Method	Location					
			LD	TC	SA	CG	LY	HC
2001	RMS	TGF-NN	–	18.57	14.37	13.47	15.71	24.77
		NAO.99b	–	17.96	13.03	9.80	16.45	13.17
	r^2	TGF-NN	–	0.845	0.878	0.950	0.860	0.648
		NAO.99b	–	0.611	0.895	0.955	0.847	0.837
2002	RMS	TGF-NN	27.46	17.61	14.19	11.73	16.79	25.18
		NAO.99b	17.05	18.71	14.26	13.76	13.55	11.46
	r^2	TGF-NN	0.537	0.856	0.861	0.923	0.836	0.629
		NAO.99b	0.703	0.596	0.883	0.907	0.890	0.874

RMS between observed tides at TC, SA, CG and LY for year 2001 and 2002 and those predicted with both models varies within a range of only 0.07–3.67 cm. For four cases TGF-NN has slightly better prediction on tides than dose NAO.99b. Contrarily, TGF-NN is worse for simulating tides than is NAO.99b for the other four cases. Applying TGF-NN to possible locations, SA, CG and LD, obtains equivalent r^2 as NAO.99b. The insignificant difference in RMS and r^2 between TGF-NN and NAO.99b shows that TGF-NN has comparably well simulating tides at a point neighboring to the original interest point and its accuracy is equivalent to that of NAO.99b.

TGF-NN has higher RMS of simulating tides at the both LD and HC than dose NAO.99b by more than 10 cm. Both points are rather far from the Hua-Lien. The F values at the TC, SA, CG and LY approximate to that of the Hua-Lien indicating tidal types are all alike at those points. However, the F values at both LD and HC are much higher than that of the Hua-Lien by 0.68 implying that the tides at both points behavior in different type from those at the Hua-Lien. Bad simulations at LD, TC and HC by TGF-NN result from time delay of tidal propagation due to bathymetrical variation on continental shelf. The topography and bathymetry around Taiwan is shown in Fig. 10. SA, HL, CG, and LY are located along the edge of continental shelf of western Pacific Ocean. LD and TC are located at the western end of Okinawa trough and separated from the other locations by Ryukyu Arc. HC is on the Heng-Chun Ridge and in shallow waters. The bathymetries of LD and HC are different from those of the other locations. TGF-NN is developed using the observed data at the Hua-Lien so that it is limited to simulate tides of different type at a point, where complex bathymetrical variation happens, far from the Hua-Lien. When the tide type, tide range or bathymetry of a position is comparably different from that of the interest point where tide data are used for training TGF-NN model, the trained TGF-NN model can not be applicable for this position, even closely neighboring to the interest point.

The hydrodynamic model used in NAO.99b needs topographical data for calculating global ocean tides and an assimilation procedure by 5 years of altimeter is used to modify the model-predicted tidal heights. TGF-NN needs only one-year astronomical data that can be easily obtained by astronomy at an interest point and used as input data and corresponding observed tidal data are used as outputs to establish TGF-NN. When astronomical data at the same point or at some point neighboring to the interest point are available, the well developed TGF-NN takes only few seconds to compute one-year tides at the point. It is accepted that TGF-NN more easily provides with accurately predicting tides at multi-points than dose NAO.99b for engineering practices.

5. Conclusions

For coastal and harbor engineering applications, it is very important to accurately calculated the tidal levels at all times.

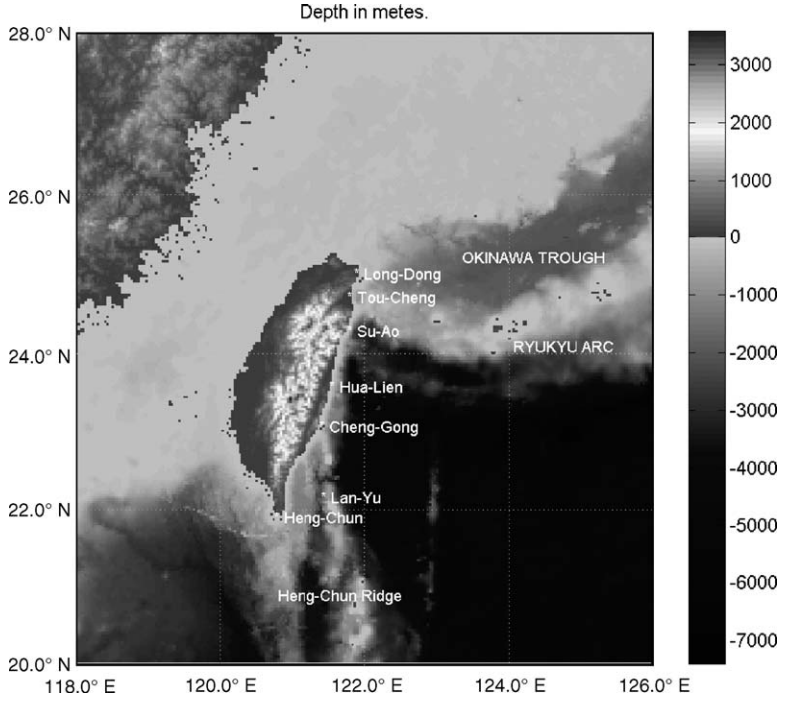

Fig. 10. The topography and bathymetry around Taiwan.

The traditional HM is restricted to tidal prediction at a single point, although its predictions are highly reliable. Based on tide theory this investigation explored an alternative TGF-NN which expresses tide-generating forces in terms of input parameters $R/D_m(t)$, $R/D_s(t)$, $R/\xi_m(t)$, $R/\xi_s(t)$, $[R/D_m(t)]^2 \cos\theta_m(t)$, $[R/D_s(t)]^2 \cos\theta_s(t)$ and $\cos\varphi(t)$. The proposed TGF-NN considers essential physical concepts of tidal propagation and tide-generating forces. The proposed model has five neurons in the hidden layer and a 2-hour lead time input, and is as powerful as HM with 60 constituents for calculating tides for a single point.

The proposed TGF-NN was applied to predict tides at points neighboring to point where the model is trained with tidal data. The predictive accuracy was compared with that of NAO.99b. The slight difference in annual RMS confirms that both methods estimate tides accurately and that the proposed TGF-NN is applicable for multi-point tidal prediction for points of which the tidal type is similar to that of the original interest point. TGF-NN is limited to simulate tides of different type and tide range at a point, where complex bathymetrical variation happens, away from the interest point where the TGF-NN model is developed.

Acknowledgment

The National Science Council, Taiwan, is greatly appreciated for providing financial support for carrying out the research under grant no. NSC 94-2611-E-009-002.

References

Atsalakis, G., Ucenic, C., Skiadas, C.H., 2005. Time series prediction of the Greek manufacturing index for the non-metallic minerals sector using a Neuro-fuzzy approach (ANFIS). Proceeding of Applied Stochastic Models and Data Analysis, pp. 1361–1369.

Chang, H.K., Chien, W.A., 2006. Neural network with multi-trend simulating transfer function for forecasting typhoon wave. Adv. Eng. Softw. 37, 184–194.

Chang, H.K., Chien, W.A., in press. A fuzzy-neural hybrid system of simulating typhoon waves. Coast. Eng. doi:10.1016/j.coastaleng.2006.02.003.

Darwin, G.H., 1907. The Harmonic Analysis of Tidal Observations in Scientific Papers, 1, Oceanic Tides and Lunar Disturbances of Gravity. Cambridge Univ. Press, London.

Demuth, H., Beale, M., 2000. Neural networks toolbox user's guide, version 4, Mathworks, Inc.

Deo, M.C., Naidu, C.S., 1998. Real time wave forecasting using neural networks. Ocean Eng. 26, 191–203.

Deo, M.C., Gondane, D.S., Kumar, V.S., 2002. Analysis of wave directional spreading using neural networks. J. Waterw. Port Coast. Ocean Eng. 128, 30–37.

Desai, S.D. 1996. Ocean tides from TOPEX/POSEIDON altimetry with some geophysical applications, Ph. D. dissertation submitted to the department of Aerospace Engineering Sciences, University of Colorado, Boulder, CO.

Desai, S.D., Wahr, J., 1995. Empirical ocean tide models estimated from TOPEX/POSEIDON altimetry. J. Geophys. Res. 100 (c12), 25205–25228.

Doodson, A.T., 1921. The harmonic development of the tide generating potential. Proc. R. Soc. Lond., A 100, 305–329.

Gill, P.R., Murray, W., Wright, M.H., 1981. The Levenberg–Marquardt Method, Practical Optimization. Academic Press, London.

Groves, G.W., Reynolds, R.W., 1975. An orthogonalized convolution method of tide prediction. J. Geophys. Res. 80, 4131–4138.

Han, G., Hendry, R., Ikeda, M., 2000. Assimilating TOPEX/POSEIDON derived tides in a primitive equation model over the Newfoundland Shelf. Cont. Shelf Res. 20, 83–108.

Kleinbaum, D.G., Kupper, L.L., Muller, K.E., 1988. Applied Regression Analysis and Other Multivariable Methods. Duxbury Press, USA.

Kumar, A., Minocha, V.K., 2001. A Discussion on Back-propagation Neural Network in Tidal-level Forecasting. In: Tsai, C.P., Lee, T.L. (Eds.), J. Wtrwy., Port, Coast., and Oc. Eng., vol. 127, pp. 54–55.

Lamb, H., 1945. Hydrodynamics, 6th ed. Dover.

Le Provost, C., Lyard, F., Molines, J.M., Genco, M.L., Rabilloud, F., 1998. A hydrodynamic ocean tide model improved by assimilating a satellite altimeter-derived data set. J. Geophys. Res. 103 (C3), 5513–5529.

Lee, T.L., 2004. Back-propagation neural network for long-term tidal predictions. Ocean Eng. 31, 225–238.

Lee, T.L., Jeng, D.S., 2002. Application of artificial neural networks in tide-forecasting. Ocean Eng. 29, 1003–1022.

Lee, T.L., Tsai, C.P., Jeng, D.S., Shieh, R.J., 2002. Neural network for prediction and supplement of tidal record in Taichung harbor, Taiwan. Adv. Eng. Softw. 33, 329–338.

Makarynskyy, O., 2004. Improving wave predictions with artificial neural networks. Ocean Eng. 31, 709–724.

Mandal, S., 2001. A Discussion on Back-propagation Neural Network in Tidal-level Forecasting. In: Tsai, C.P., Lee, T.L. (Eds.), J. Wtrwy., Port, Coast., and Oc. Eng., vol. 127, pp. 54–55.

Matsumoto, K., Takanezawa, T., Ooe, M., 2000. Ocean tide model developed by assimilating TOPEX/POSEIDON altimetry data into hydrodynamical model: a global and a regional model around Japan. J. Oceanogr. 56, 567–581.

Medina, J.R., 2001. A Discussion on Back-propagation Neural Network in Tidal-level Forecasting. In: Tsai, C.P., Lee, T.L. (Eds.), J. Wtrwy., Port, Coast., and Oc. Eng., vol. 127, pp. 55–57.

Munk, W.H., Cartwright, D.E., 1996. Tidal spectroscopy and prediction. Philos. Trans. R. Soc. Lond. Ser. A 259, 533–581.

Ray, R.D., 1998. Spectral analysis of highly aliased sea-level signals. J. Geophys. Res. 103 (C11), 24991–25003.

Tsai, C.P., Lee, T.L., 1999. Back-propagation neural network in tidal-level forecasting. J. Waterw. Port Coast. Ocean Eng. 125, 195–202.

Vaziri, M., 1997. Predicting Caspian Sea surface water level by ANN and ARIMA models. J. Waterw. Port Coast. Ocean Eng. 123, 158–162.

Walton, T.L., Garcia, A.W., 2001. A Discussion on Back-propagation Neural Network in Tidal-level Forecasting. In: Tsai, C.P., Lee, T.L. (Eds.), J. Wtrwy., Port, Coast., and Oc. Eng., vol. 127, pp. 57–58.